IEEE Access
Multidisciplinary | Rapid Review | Open Access Journal

Received January 9, 2019, accepted January 28, 2019, date of publication February 1, 2019, date of current version February 27, 2019.

Digital Object Identifier 10.1109/ACCESS.2019.2896996

Field-Programmable Gate Array-Based Coating Impedance Detector for Rapid Evaluation of Early Degradation of Protective Coatings

YUEH-LIEN LEE, YU-TONG KUO, HUNG-HSUN CHEN, AND YUNG-AN HSIEH
Department of Engineering Science and Ocean Engineering, National Taiwan University, Taipei 10617, Taiwan

Corresponding author: Yueh-Lien Lee (yuehlien@ntu.edu.tw)

This work was supported in part by the Ministry of Science and Technology, R.O.C, under Grant MOST 106-2221-E-002-237 and in part by the Ship and Ocean Industries R&D Center.

ABSTRACT In this paper, a novel, compact, And field-programmable gate array (FPGA)-based coating impedance detector (CID 2.0) was proposed to rapidly detect the early degradation of coatings. An FPGA-based hardware design with an embedded analog-to-digital converter and digital-to-analog converter was successfully applied to develop CID 2.0. A method for generating high-quality signals for FPGA by using the delta–sigma modulation was used. This method provided higher measurement ranges and accuracies for detecting coating impedance values. The performance of CID 2.0 was compared with that of a conventional potentiostat. For comparison, the impedance value of ideal resistors and commercial coatings was measured using the proposed and conventional methods. The results indicated an optimal correlation between the impedance values measured using CID 2.0 and that measured using conventional potentiostat in the range of $10^6 - 10^{10}$ Ω-cm^2. Furthermore, when the continuous monitoring experiments were conducted, CID 2.0 exhibited high sensitivity to detect impedance changes associated with the coating delamination process. The preliminary results suggested that CID 2.0 can be used to observe the changes in the coating impedance values in the critical range to enable workers to determine whether coating maintenance should be scheduled.

INDEX TERMS Coating, corrosion monitor, electrochemical impedance spectroscopy, impedance measurement, field-programmable gate array.

I. INTRODUCTION

Metallic materials are usually susceptible to corrosion on exposure to a moist-air environment. Therefore, several methods have been developed to prevent corrosion or to control the rate of corrosion. Among the various corrosion protection methods, the application of an organic coating on the surface of the metal is considered as the most effective and economical method for providing a physical barrier against corrosion. However, most organic coatings are permeable to water and oxygen; thus, they cannot provide permanent corrosion protection for the metals. The durability of organic coating has been causing a considerable concern among many researchers for many years. Therefore, it is crucial to understand the deterioration rate of organic coating so that preventive maintenance could be scheduled to prolong the service life of metals. Electrochemical impedance spectroscopy (EIS) conducted using a potentiostat has been considered as a reliable and nondestructive technique for determining the service life of protective coatings [1]–[14]. However, this method is not suitable for field measurements because it has several limitations, including the following: (1) most potentiostats are bulky and expensive, (2) additional instruments such as counter and reference electrodes are required for the EIS measurement, and (3) potentiostats require a large power source for operation. As a result, the attempts to modify the traditional EIS experimental setup have been increasing. Researchers have invested considerable efforts to develop a simplified monitoring system based on EIS for predicting the protective performance of organic coatings during the past 20 years [5], [15]–[38]. For example, Carullo *et al.* [24]–[26] designed a low-cost and portable EIS

The associate editor coordinating the review of this manuscript and approving it for publication was Dinesh Thanu.

system based on digital signal processor boards. The device can measure impedances up to 1 GΩ with an error of less than 4% in magnitude and 1° in phase. Several researchers have designed low-cost EIS systems for corrosion monitoring [27]–[29]. Angelini *et al.* [30] described a portable impedance device for coating. The measurement range of the device was from a few kilo-ohms to several tens of gigaohms with an error of approximately 3%. Subsequently, the authors modified the experimental setup and proposed an Arduino-based EIS instrument with a logarithmic amplifier [30]. The results revealed that the instrument can measure in the range of 1kΩ-1GΩ with an error of approximately 2%. However, the accuracy was expressed in the laboratory by using a known capacitor and resistor. The authors selected a very-wide frequency range (0.1 Hz–10 kHz) to obtain the complete impedance spectrum. This solution is effective and can achieve equivalent circuit modeling; however, it increases the measurement time. Davis *et al.* [31]–[38] began developing a coating health monitor (CHM) for Army ground vehicles in 1999. The CHM was designed to measure impedance by using three frequencies (0.2, 0.5, and 0.9 Hz). The efficiency of the CHM was compared with that of the commercial Gamry potentiostat (Warminster, PA, USA) by using a resistor–capacitor circuit and a coated specimen. The results of the CHM were similar to those of the Gamry potentiostat [38]. Although the CHM is a battery-powered, wireless microsensor system with the EIS function, it may not be suitable for on-site monitoring because of its high cost and limited performance (CHM cannot measure a coating with impedance more than 5×10^8 Ω-cm^2.)

In our previous research, a coating impedance detector (CID) was proposed for rapid evaluation of the protective properties of coatings [39]. The size of the CID was designed and set to $4 \times 4 \times 0.1$ cm^3 so that it can be easily applied to on-field applications. However, the first version of the CID is not a complete system and is only a concept-proving prototype. A signal source and oscilloscope were required to complete the measurement in the previous study. Moreover, in the first version of the CID, we only focused on the accurate detection of variation in the coating impedance value in the range of $10^7 - 10^9$ Ω-cm^2, which encompasses values of only one order higher than and one order lower than 10^8 Ω-cm^2 (a specified impedance value threshold for good coatings). Thus, in this study, an Altera DE0-Nano field-programmable gate array (FPGA) microcontroller was used for developing an innovative, compact coating impedance detector (CID 2.0). A method for generating high-quality signals for the FPGA by using the delta-sigma modulation was applied to provide low-noise and low-signal amplitudes, which are usually required in electrochemical analysis applications. As a result, a practical miniaturized detector with a higher working range and accuracies could be obtained. The impedance of the commercial epoxy-coated samples measured using CID 2.0 were compared with the impedance of the samples measured using the conventional potentiostat. Continuous monitoring experiments were conducted to demonstrate the efficiency of CID 2.0 to monitor the coating degradation.

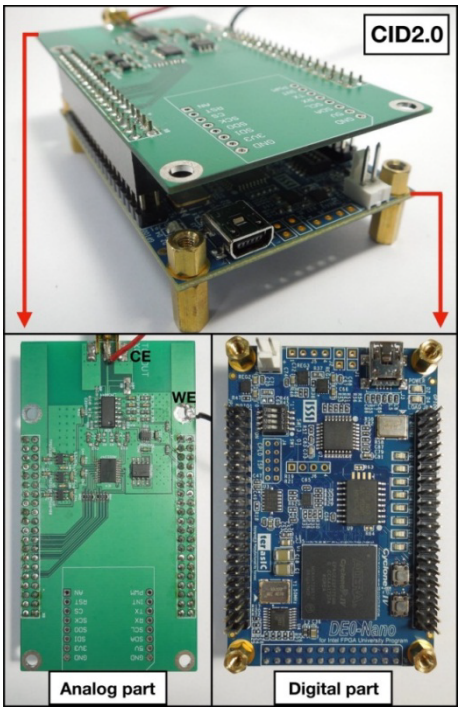

FIGURE 1. Photograph of CID 2.0.

II. SYSTEM DESIGN

As displayed in Fig. 1, the hardware of CID 2.0 has two parts-the digital and analog parts. The digital part contained a commercially available FPGA development board (DE0-Nano board with an Altera Cyclone IV FPGA). The analog part contained a custom-made printed circuit board with a pair of analog-to-digital converters (ADCs), a pair of unity-gain buffers, an active low-pass filter (LPF), and power supply circuit. The FPGA was used to implement a numerically controlled oscillator that was used to generate sinusoidal signals that are required for Fourier analysis and excitation signal generation. A single-bit delta-sigma ($\Delta\Sigma$) digital-to-analog converter was also implemented inside the FPGA, which outputs a 1-bit bitstream to the active LPF on the analog board. After filtering with the LPF, the output is a continuous 10-mV sinusoidal signal and is presented as v1 in Fig. 2 with a tunable frequency. In previous studies, many researchers have conducted characteristic frequency analysis to rapidly assess the coating performance [39]. Furthermore, the impedance value at a low-frequency range in Bode plots is a crucial indicator of the coating performance. Consequently, the impedance value evaluated at a characteristic frequency of 1 Hz (i.e., $|Z|_{1\text{Hz}}$) was selected for all CID 2.0 measurements. The reference resistor (Z_{ref}) and equivalent coating impedance (Z_c) together form an impedance divider. The voltage v2 is the voltage between Z_{ref} and Z_c.

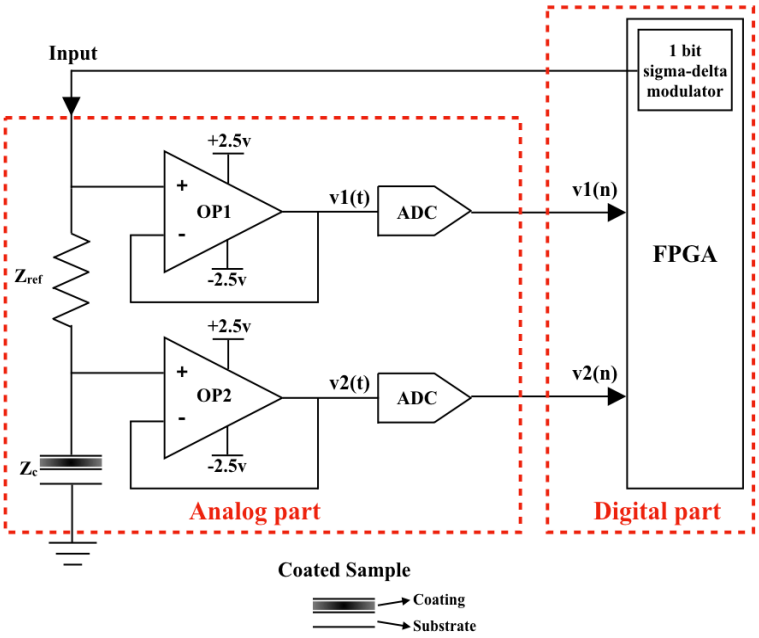

FIGURE 2. Block diagram of CID 2.0.

According to Kirchoff's law, the relationship between the V_1 and V_2 is given as follows:

$$V_2(1\text{ Hz}) = V_1(1\text{ Hz})\frac{\text{Zc}(1\text{ Hz})}{Zref + Zc(1\text{Hz})} \quad (1)$$

where V_1(1 Hz) and V_2(1 Hz) are the Fourier transforms of v1 and v2 at 1 Hz, respectively. As the input impedance of ADCs is usually considerably smaller than the impedance of Z_c, a pair of unity-gain buffers was inserted before the ADCs. The input impedance of the unity-gain buffers is considerably large; thus, v1 and v2 are not affected by loading effects. The pair of voltages—v1 and v2—are digitized and sent to the FPGA. The FPGA performs Fourier transform on v1 and v2 at a frequency of 1 Hz to obtain the V_1 and V_2 values.

III. EXPERIMENTAL PROCEDURE

In this study, ideal high-value resistors and epoxy-coated samples with various impedance values in the range of $10^5 - 10^9$ Ω-cm^2, including steel substrates with an epoxy coating of different thicknesses (50, 100, and 250 μm), blistered epoxy coated samples and high-performance commercial coated samples, were fabricated to verify the accuracy and performance range of the proposed device. The impedance was also measured using the conventional potentiostat (Gamry Reference 600) for comparison in this study. The potentiostat with a standard three-electrode setup was used, which comprised the coated sample as the working electrode (WE), a saturated calomel reference electrode (RE), and a graphite rod as the counter electrode (CE). CID 2.0 was used with a simplified two-electrode setup, which is more suitable for installation in the field. The exposed surface area of the coated sample was 7.8 cm^2, and the working electrolyte was a 3.5 wt.% NaCl solution. The comparison between the measurement configuration of CID and CID 2.0 is presented in Fig. 3.

IV. RESULTS AND DATA ANALYSIS

A. MEASUREMENT EFFICIENCY

First, the measurement efficiency of CID 2.0 was evaluated by measuring ideal resistors that were in the range of 0.1 MΩ to 1 GΩ. The impedance value of various ideal resistors measured using CID 2.0 and the conventional potentiostat is summarized in Table 1. The impedance values obtained by the CID 2.0 and potentiostat in the Table 1 are the mean value of 10 measurements. Table 1 presents the $|Z|$ values of five ideal resistors measured using CID 2.0 – 1.04×10^5, 1.00×10^6, 1.01×10^7, 1.00×10^8 and 9.91×10^8 Ω. Optimal correlation with minimal differences was observed between the outputs of CID 2.0 and the conventional potentiostat while measuring the impedance value of the ideal resistors. It should be noted that CID 2.0 exhibited less variation in the quality of data (9.91×10^8 Ω) on measuring the impedance value of 1 GΩ ideal resistors compared with that measured by previous CID version (7.62×10^8 Ω). This suggested CID 2.0 allowed more accurate estimates to be made.

The impedance spectra (i.e., Bode magnitude plots) of the EIS measurements for the four coatings are depicted in Fig. 4. The solid black line for the wide frequency range in the Bode magnitude plot represents the impedance data measured using the conventional potentiostat, and the red point with an error bar at 1 Hz indicates the average of the five $|Z|_{1\text{Hz}}$ values measured using CID 2.0. As displayed in the Fig. 4(a),

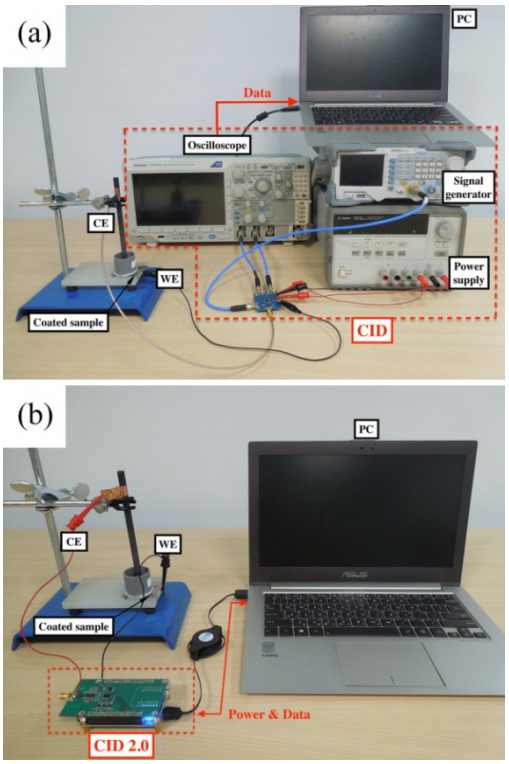

FIGURE 3. Comparison of the measurement configuration between (a) CID and (b) CID 2.0.

the $|Z|_{1\text{Hz}}$ value of the 50-μm-thick epoxy-coated sample measured using the potentiostat was 9.98×10^8 Ω-cm^2. The average of five $|Z|_{1\text{Hz}}$ values measured using CID 2.0 for the same coated sample was 9.75×10^8 Ω-cm^2, with a small standard deviation (9.43×10^7 Ω-cm^2). In Fig. 4(b), the $|Z|_{1\text{Hz}}$ value of the 100-μm-thick epoxy-coated sample measured by the potentiostat was 3.97×10^9 Ω-cm^2. The average of five $|Z|_{1\text{Hz}}$ values obtained using CID 2.0 for the same coated sample was $3.81 \times 10^9 \pm 5.80 \times 10^7$ Ω-cm^2. The measurement results obtained using CID 2.0 and the potentiostat for the two epoxy coatings were in agreement with each other. Noticeably, for the coated samples with a higher impedance value ($> 10^{10}$ Ω-cm^2), the $|Z|_{1\text{Hz}}$ value measured using the potentiostat was 1.84×10^{10} Ω-cm^2. In our previous study, some variation was observed in the impedance values obtained from these two measurements when a high-quality coated sample (impedance value $>10^{10}$ Ω-cm^2) was selected for testing. However, as presented in Fig. 4(c), the $|Z|_{1\text{Hz}}$ value obtained using CID 2.0 ($1.78 \times 10^{10} \pm 6.42 \times 10^8$ Ω-cm^2) was similar to that obtained using the potentiostat. The coated samples with lower impedance value ($<10^7$ Ω-cm^2) were also fabricated and tested. As presented in Fig. 4(d), the $|Z|_{1\text{Hz}}$ value of the blistered epoxy coated sample measured using the potentiostat was 8.66×10^6 Ω-cm^2. In our previous study, a slight offset between the outputs of CID and the potentiostat was observed when a damaged coating with lower impedance values was considered. By contrast, slight or no variation was observed in the quality of the data obtained using CID 2.0 ($8.11 \times 10^6 \pm 1.04 \times 10^5$ Ω-cm^2) compared with that

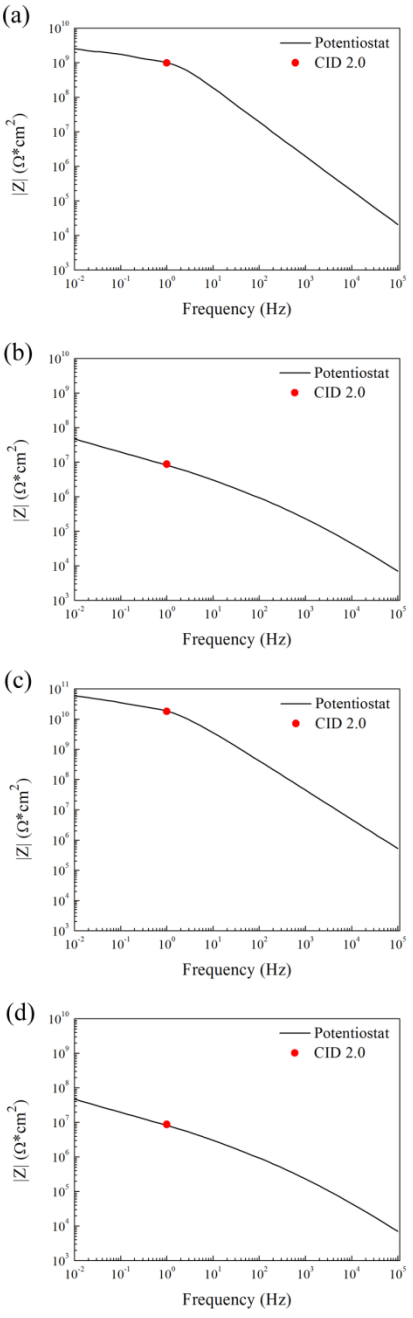

FIGURE 4. Comparison of the results between CID 2.0 and the conventional potentiostat when (a) a 50-μm-thick epoxy-coated sample, (b) 100-μm-thick epoxy-coated sample, (c) high-performance commercial coated sample, and (d) blistered epoxy coated sample are used.

obtained using the potentiostat, as presented in Fig. 4(d). Overall, the performance of the proposed device—CID 2.0—is comparable to that of CID. Moreover, the accuracy of CID 2.0 of estimating the $|Z|_{1\text{Hz}}$ values of high-quality and damaged coatings is higher than the accuracy of CID.

B. ANALYSIS OF THE CORROSION MONITORING RESULTS

After demonstrating the validity of the results obtained using CID 2.0, it was necessary to identify whether CID 2.0 can be

TABLE 1. Measurement data of CID 2.0 and the conventional potentiostat.

(unit: Ω)

Resistor	0.1M Ω	1M Ω	10M Ω	100M Ω	1G Ω
Potentiostat $\|Z\|_{1Hz}$	$9.93*10^4$	$9.98*10^5$	$1.00*10^7$	$1.02*10^8$	$1.00*10^9$
CID 2.0	$1.04*10^5$	$1.00*10^6$	$1.01*10^7$	$1.00*10^8$	$9.91*10^8$
CID 2.0 Standard deviation	$1.14*10^3$	$2.65*10^3$	$2.66*10^4$	$4.44*10^5$	$4.01*10^7$

TABLE 2. Comparison of the results between CID 2.0 and the conventional potentiostat for a duration of 28 h.

(unit: $\Omega*cm^2$)

Sample	1 h	18 h	20 h	24 h	28 h
Potentiostat $\|Z\|_{1Hz}$	$6.25*10^9$	$4.56*10^9$	$2.75*10^9$	$1.36*10^9$	$2.85*10^7$
CID 2.0	$6.24*10^9$	$4.54*10^9$	$2.54*10^9$	$1.24*10^9$	$3.14*10^7$
CID 2.0 standard deviation	$3.10*10^8$	$2.80*10^8$	$1.08*10^8$	$4.62*10^8$	$3.82*10^6$

applied in situ to monitor the decrease in the low-frequency impedance value related to coating degradation. In this experiment, a 250-μm-thick epoxy-coated sample was fabricated and 3.5 wt.% NaCl solution with 10^{-4} mole of sulfuric acid was used as the test solution because the coated samples likely degrade in a short test time in this environment. Coating degradation monitoring was conducted using both CID 2.0 and the potentiostat. The results from these two methods were combined in one figure for comparison.

Fig. 5 displays the Bode plots measured using the potentiostat (color solid line) and time-dependent impedance value (color points) measured using CID 2.0 for 28 h of immersion. Usually, the epoxy coating exhibited almost a straight line with high impedance value (more than 10^{10} Ω-cm^2 at the lowest frequency of 10^{-2} Hz) in the Bode plots at the beginning of the test, thus indicating its excellent barrier properties maintains a highly capacitive behavior in neutral solution. However, the Bode plots presented a horizontal line after the first hour of immersion. This line formation can be attributed to the resistive behavior corresponding to the charge transfer reaction and corrosion process occurring at the coating–substrate interface, demonstrating the early degradation of epoxy coating exposed to acidic environments. Notably, a significant decrease in low-frequency impedance values was observed in the first 24 h of immersion, and further deterioration and gradual decrease in impedance values below 10^8 Ω-cm^2 were observed after 28 h of immersion. This implied that the loss of barrier properties corresponded to the penetration of water and electrolyte through the pores

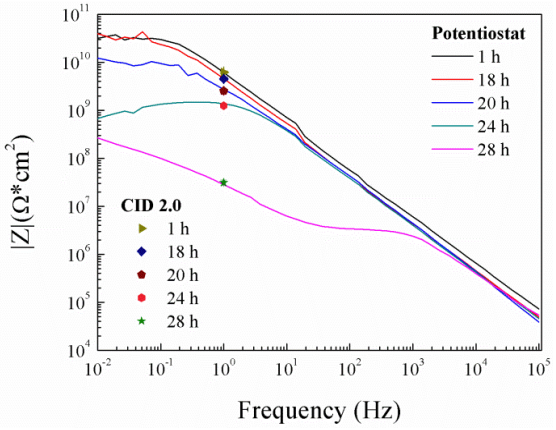

FIGURE 5. Corrosion monitoring results of a 250-μm-thick epoxy-coated sample when the conventional potentiostat and CID 2.0 are used.

and defects of the coating up to the metal [40]. A similar trend was detected in the color points marked on the frequency plot of 1 Hz. This data demonstrated a high correlation between the two methods, thus suggesting that CID 2.0 has a higher probability of detecting damage in the coating and is suitable for coating degradation monitoring. Table 2 summarizes the $|Z|_{1Hz}$ values obtained using CID 2.0 and the potentiostat for the 28 h test. Overall, although the CID 2.0 is not able to have detailed performance assessment of coatings and provide kinetic information regarding the corrosion process, it is extremely useful to monitor the changes in the coating impedance values in the critical range to help maintenance

engineers determine whether coating maintenance should be scheduled. Finally, for the practical aspects and future application of use of CID 2.0 in the field, a shield box, which is used to enclose CID 2.0 should be designed and employed.

V. CONCLUSIONS

An FPGA-based CID 2.0 was proposed and characterized in this study for rapid detection of the early degradation of coatings. The oscilloscope and signal generator used in the previous CID version were successfully simplified and integrated in CID 2.0 by using an FPGA-based hardware design. Consequently, a novel, miniaturized coating impedance detector with a dimension of $5\,\text{cm} \times 9\,\text{cm} \times 1.6\,\text{mm}$ was developed. The consistency between the impedance values measured using CID 2.0 and the conventional potentiostat for a given coating in the range of $10^6 - 10^{10}\ \Omega\text{-cm}^2$ demonstrated the reliability of CID 2.0. CID 2.0 also exhibited an excellent ability to monitor the decrease in the impedance values at a low frequency that is associated with the degradation of coatings during the continuous immersion test. The estimated accuracy of CID 2.0 is higher when measurements are conducted on the 10^6 and more than $10^{10}\ \Omega\text{-cm}^2$ grade coatings, thus extending the applicability of CID 2.0 to monitor material degradation.

ACKNOWLEDGMENT

The authors would like to thank Dr. Jau-Horng Chen and Dr. Cheng-Hsien Chung for the technical assistance and valuable advice.

REFERENCES

[1] E. Cano, A. Crespo, D. Lafuente, and B. R. Barat, "A novel gel polymer electrolyte cell for *in-situ* application of corrosion electrochemical techniques," *Electrochem. Commun.*, vol. 41, pp. 16–19, Apr. 2014.

[2] A. Collazo, R. Figueroa, X. R. Nóvoa, and C. Pérez, "Corrosion of electrodeposited Sn in 0.01 M NaCl solution. A EQCM and EIS study," *Electrochim. Acta*, vol. 202, pp. 288–298, Jun. 2016.

[3] A. de Vooys and H. van der Weijde, "Investigating cracks and crazes on coated steel with simultaneous SVET and EIS," *Prog. Organic Coat.*, vol. 71, pp. 250–255, Jul. 2011.

[4] J. C. S. Fernandes, A. Nunes, M. J. Carvalho, and T. C. Diamantino, "Degradation of selective solar absorber surfaces in solar thermal collectors—An EIS study," *Sol. Energy Mater. Sol. Cells*, vol. 160, pp. 149–163, Feb. 2017.

[5] M. Kendig and J. Scully, "Basic aspects of electrochemical impedance application for the life prediction of organic coatings on metals," *Corrosion*, vol. 46, pp. 22–29, Jan. 1990

[6] D. D. Macdonald, "Some advantages and pitfalls of electrochemical impedance spectroscopy," *Corrosion*, vol. 46, pp. 229–242, Mar. 1990.

[7] Y. A. N. Maocheng, X. U. Jin, Y. U. Libao, W. U. Tangqing, S. U. N. Cheng, and K. E. Wei, "EIS analysis on stress corrosion initiation of pipeline steel under disbonded coating in near-neutral pH simulated soil electrolyte," *Corrosion Sci.*, vol. 110, pp. 23–34, Sep. 2016.

[8] J. N. Murray and H. P. Hack, "Testing organic architectural coatings in ASTM synthetic seawater immersion conditions using EIS," *Corrosion*, vol. 48, pp. 671–685, Aug. 1992.

[9] B. R. Barat, A. Crespo, E. García, S. Díaz, and E. Cano, "An EIS study of the conservation treatment of the bronze sphinxes at the Museo Arqueológico Nacional (Madrid)," *J. Cultural Heritage*, vol. 24, pp. 93–99, Mar./Apr. 2017.

[10] D. V. Ribeiro and J. C. C. Abrantes, "Application of electrochemical impedance spectroscopy (EIS) to monitor the corrosion of reinforced concrete: A new approach," *Construction Building Mater.*, vol. 111, pp. 98–104, May 2016.

[11] J. Titz, G. H. Wagner, H. Spähn, M. Ebert, K. Jüttner, and W. J. Lorenz, "Characterization of organic coatings on metal substrates by electrochemical impedance spectroscopy," *Corrosion*, vol. 46, pp. 221–229, May 1990.

[12] M. A. Varnosfaderani and D. Strickland, "Online Electrochemical Impedance Spectroscopy (EIS) estimation of a solar panel," *Vacuum*, vol. 139, pp. 185–195, May 2017.

[13] Z. Wang, J. Li, Y. Wang, and Z. Wang, "An EIS analysis on corrosion resistance of anti-abrasion coating," *Surfaces Interfaces*, vol. 6, pp. 33–39, Mar. 2017.

[14] X. Yuan, Z. F. Yue, X. Chen, S. F. Wen, L. Li, and T. Feng, "EIS study of effective capacitance and water uptake behaviors of silicone-epoxy hybrid coatings on mild steel," *Prog. Organic Coat.*, vol. 86, pp. 41–48, Sep. 2015.

[15] S. Ahmad, "Reinforcement corrosion in concrete structures, its monitoring and service life prediction—A review," *Cement Concrete Compos.*, vol. 25, pp. 459–471, May/Jun. 2003.

[16] K. Al Handawi, N. Vahdati, P. Rostron, L. Lawand, and O. Shiryayev, "Strain based FBG sensor for real-time corrosion rate monitoring in pre-stressed structures," *Sens. Actuators B, Chem.*, vol. 236, pp. 276–285, Nov. 2016.

[17] F. Gan, G. Tian, Z. Wan, J. Liao, and W. Li, "Investigation of pitting corrosion monitoring using field signature method," *Measurement*, vol. 82, pp. 46–54, Mar. 2016.

[18] J. Jiang *et al.*, "Smartphone based portable bacteria pre-concentrating microfluidic sensor and impedance sensing system," *Sens. Actuators B, Chem.*, vol. 193, pp. 653–659, Mar. 2014.

[19] K. Subbiah, S. Velu, S.-J. Kwon, H.-S. Lee, N. Rethinam, and D.-J. Park, "A novel *in-situ* corrosion monitoring electrode for reinforced concrete structures," *Electrochim. Acta*, vol. 259, pp. 1129–1144, Jan. 2018.

[20] S. Muralidharan, T. H. Ha, J. H. Bae, Y. C. Ha, H. G. Lee, and D. K. Kim, "A promising potential embeddable sensor for corrosion monitoring application in concrete structures," *Measurement*, vol. 40, pp. 600–606, Jul. 2007.

[21] J. Orlikowski, K. Darowicki, and S. Mikolajski, "Multi-sensor monitoring of the corrosion rate and the assessment of the efficiency of a corrosion inhibitor in utility water installations," *Sens. Actuator B, Chem.*, vol. 181, pp. 22–28, May 2013.

[22] H. Zhang, R. Yang, Y. He, G. Y. Tian, L. Xu, and R. Wu, "Identification and characterisation of steel corrosion using passive high frequency RFID sensors," *Measurement*, vol. 92, pp. 421–427, Oct. 2016.

[23] X. Zou, T. Schmitt, D. Perloff, N. Wu, T.-Y. Yu, and X. Wang, "Non-destructive corrosion detection using fiber optic photoacoustic ultrasound generator," *Measurement*, vol. 62, pp. 74–80, Feb. 2015.

[24] A. Carullo, F. Ferraris, M. Parvis, A. Vallan, E. Angelini, and P. Spinelli, "Low-cost electrochemical impedance spectroscopy system for corrosion monitoring of metallic antiquities and works of art," *IEEE Trans. Instrum. Meas.*, vol. 49, no. 2, pp. 371–375, Apr. 2000.

[25] E. Angelini *et al.*, "Handheld-impedance-measurement system with seven-decade capability and potentiostatic function," *IEEE Trans. Instrum. Meas.*, vol. 55, no. 2, pp. 436–441, Apr. 2006.

[26] A. Carullo, S. Corbellini, M. Parvis, and A. Vallan, "A wireless sensor network for cold-chain monitoring," *IEEE Trans. Instrum. Meas.*, vol. 58, no. 5, pp. 1405–1411, May 2009.

[27] S. Grassini, S. Corbellini, E. Angelini, F. Ferraris, and M. Parvis, "Low-cost impedance spectroscopy system based on a logarithmic amplifier," *IEEE Trans. Instrum. Meas.*, vol. 64, no. 5, pp. 1110–1117, May 2015.

[28] S. Corbellini, M. Parvis, and S. Grassini, "Noninvasive solution for electrochemical impedance spectroscopy on metallic works of art," *IEEE Trans. Instrum. Meas.*, vol. 61, no. 5, pp. 1193–1200, May 2012.

[29] S. Grassini, S. Corbellini, M. Parvis, E. Angelini, and F. Zucchi, "A simple Arduino-based EIS system for *in situ* corrosion monitoring of metallic works of art," *Measurement*, vol. 114, pp. 508–514, Jan. 2018.

[30] E. Angelini, S. Corbellini, M. Parvis, F. Ferraris, and S. Grassini, "An Arduino-based EIS with a logarithmic amplifier for corrosion monitoring," in *Proc. IEEE Int. Instrum. Meas. Technol. Conf.*, May 2014, pp. 905–910.

[31] G. D. Davis, L. A. Krebs, L. T. Drzal, M. J. Rich, and P. Askeland, "Electrochemical sensors for nondestructive evaluation of adhesive bonds," *J. Adhes.*, vol. 72, nos. 3–4, pp. 335–358, 2000.

[32] G. D. Davis and J. G. Dillard, "Development of an electrochemical impedance spectroscopy sealant test: II. Conductive sealants," *J. Adhes. Sci. Technol.*, vol. 20, no. 11, pp. 1235–1253, 2006.

[33] G. D. Davis and J. G. Dillard, "Development of an electrochemical impedance spectroscopy sealant test: I. Nonconductive sealants," *J. Adhes. Sci. Technol.*, vol. 20, no. 11, pp. 1215–1233, 2006.

[34] G. D. Davis, S. Mani, M. J. Rich, and L. T. Drzal, "Electrochemical impedance spectroscopy inspection of composite adhesive joints," *J. Adhes. Sci. Technol.*, vol. 19, no. 6, pp. 467–492, 2005.
[35] G. D. Davis, R. A. Pethrick, and J. Doyle, "Detection of moisture in adhesive bonds using electrochemical impedance and dielectric spectroscopies," *J. Adhes. Sci. Technol.*, vol. 23, no. 4, pp. 507–528, 2009.
[36] G. D. Davis, K. Thayer, M. J. Rich, and L. T. Drzal, "Inspection of composite and metal adhesive bonds with an electrochemical sensor," *J. Adhes. Sci. Technol.*, vol. 16, no. 10, pp. 1307–1326, 2002.
[37] G. Davis, T. G. Vargo, A. W. Dalgleish, and D. Deason, "Corrosion protection and condition monitoring using 'Smart' appliques," *Mater. Perform.*, vol. 43, pp. 32–36, Aug. 2004.
[38] G. Davis, R. Dunn, R. Ros, "Wireless, battery-powered coating health monitor (CHM)," in *Proc. Int. Corrosion Conf. Ser. (NACE)*, 2010, pp. 1–9.
[39] Y.-T. Kuo, C.-Y. Lee, and Y.-L. Lee, "Compact coating impedance detector for fast evaluation of coating degradation," *Measurement*, vol. 124, pp. 303–308, Aug. 2018.
[40] Y. González-García, S. González, and R. M. Souto, "Electrochemical and structural properties of a polyurethane coating on steel substrates for corrosion protection," *Corrosion Sci.*, vol. 49, pp. 3514–3526, Sep. 2007.

YUEH-LIEN LEE received the B.S. and M.S. degrees in mechanical engineering from National Central University, Taoyuan, in 2004 and 2005, respectively, and the Ph.D. degree in materials science and engineering from National Taiwan University, Taipei, in 2011. From 2011 to 2014, he was a Postdoctoral Fellow with the Fontana Corrosion Center, Department of Materials Science and Engineering, The Ohio State University, Columbus, OH, USA, where he was involved in electrochemistry of corrosion, corrosion prediction, and corrosion protection. In 2014, he joined National Taiwan University, where he is currently an Assistant Professor with the Department of Engineering Science and Ocean Engineering. His research interests include corrosion monitoring, surface modification, and corrosion resistant coatings.

YU-TONG KUO received the B.S. degree in physics from National Chung Cheng University, Chiayi, in 2016, and the M.S. degree in engineering science and ocean engineering from National Taiwan University, Taipei, in 2018. She is currently a Technology Development Engineer with InnoLux Corporation, Tainan, Taiwan.

HUNG-HSUN CHEN received the B.S. degree in system engineering and naval architecture from National Taiwan Ocean University, Keelung, in 2017. He is currently pursuing the M.S. degree in engineering science and ocean engineering with National Taiwan University, Taipei, Taiwan.

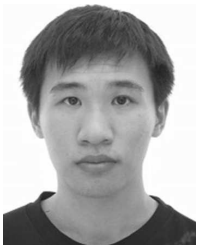

YUNG-AN HSIEH received the B.S. degree *(summa cum laude)* from the Department of Engineering Science and Ocean Engineering, National Taiwan University, Taipei, Taiwan, in 2017. He is currently pursuing the Ph.D. degree with the School of Electrical and Computer Engineering, Georgia Institute of Technology, Atlanta, GA, USA. His research interests include digital signal processing and embedded systems.